Commissioning of the Varian TrueBeam linear accelerator: A multi-institutional study

C. Glide-Hurst[a] and M. Bellon
Department of Radiation Oncology, Henry Ford Health Systems, Detroit, Michigan 48202

R. Foster
Department of Radiation Oncology, The University of Texas Southwestern Medical Center, Dallas, Texas 75235

C. Altunbas
Department of Radiation Oncology, University of Colorado School of Medicine, Aurora, Colorado 80045

M. Speiser
Department of Radiation Oncology, The University of Texas Southwestern Medical Center, Dallas, Texas 75235

M. Altman
Department of Radiation Oncology, Washington University School of Medicine, St. Louis, Missouri 63110

D. Westerly
Department of Radiation Oncology, University of Colorado School of Medicine, Aurora, Colorado 80045

N. Wen and B. Zhao
Department of Radiation Oncology, Henry Ford Health Systems, Detroit, Michigan 48202

M. Miften
Department of Radiation Oncology, University of Colorado School of Medicine, Aurora, Colorado 80045

I. J. Chetty
Department of Radiation Oncology, Henry Ford Health Systems, Detroit, Michigan 48202

T. Solberg
Department of Radiation Oncology, The University of Texas Southwestern Medical Center, Dallas, Texas 75235

(Received 5 July 2012; revised 18 January 2013; accepted for publication 23 January 2013; published 1 March 2013)

Purpose: Latest generation linear accelerators (linacs), i.e., TrueBeam (Varian Medical Systems, Palo Alto, CA) and its stereotactic counterpart, TrueBeam STx, have several unique features, including high-dose-rate flattening-filter-free (FFF) photon modes, reengineered electron modes with new scattering foil geometries, updated imaging hardware/software, and a novel control system. An evaluation of five TrueBeam linacs at three different institutions has been performed and this work reports on the commissioning experience.

Methods: Acceptance and commissioning data were analyzed for five TrueBeam linacs equipped with 120 leaf (5 mm width) MLCs at three different institutions. Dosimetric data and mechanical parameters were compared. These included measurements of photon beam profiles (6X, 6XFFF, 10X, 10XFFF, 15X), photon and electron percent depth dose (PDD) curves (6, 9, 12 MeV), relative photon output factors (Scp), electron cone factors, mechanical isocenter accuracy, MLC transmission, and dosimetric leaf gap (DLG). End-to-end testing and IMRT commissioning were also conducted.

Results: Gantry/collimator isocentricity measurements were similar (0.27–0.28 mm), with overall couch/gantry/collimator values of 0.46–0.68 mm across the three institutions. Dosimetric data showed good agreement between machines. The average MLC DLGs for 6, 10, and 15 MV photons were 1.33 ± 0.23, 1.57 ± 0.24, and 1.61 ± 0.26 mm, respectively. 6XFFF and 10XFFF modes had average DLGs of 1.16 ± 0.22 and 1.44 ± 0.30 mm, respectively. MLC transmission showed minimal variation across the three institutions, with the standard deviation $<0.2\%$ for all linacs. Photon and electron PDDs were comparable for all energies. 6, 10, and 15 MV photon beam quality, $\%dd(10)_x$ varied less than 0.3% for all linacs. Output factors (Scp) and electron cone factors agreed within 0.27%, on average; largest variations were observed for small field sizes (1.2% coefficient of variation, 10 MV, 2×2 cm^2) and small cone sizes ($<1\%$ coefficient of variation, 6×6 cm^2 cone), respectively.

Conclusions: Overall, excellent agreement was observed in TrueBeam commissioning data. This set of multi-institutional data can provide comparison data to others embarking on TrueBeam commissioning, ultimately improving the safety and quality of beam commissioning. © *2013 American Association of Physicists in Medicine*. [http://dx.doi.org/10.1118/1.4790563]

Key words: commissioning, linear accelerator, dosimetric parameters

I. INTRODUCTION

One of the latest generations of linear accelerator (linac), the TrueBeam (Varian Medical Systems, Palo Alto, CA) and its stereotactic counterpart, the TrueBeam STx, have different characteristics than previous linear accelerators. These include: several high dose rate flattening-filter-free (FFF) photon modes, reengineered electron modes with new scattering foil geometry, and updated imaging hardware and software. While the dosimetric characteristics of the TrueBeam STx (Varian Medical Systems, Palo Alto, CA) FFF modes have been aptly described in the literature, the STx houses the high-definition multileaf collimator (HDMLC) with smaller leaf projection at isocenter.[1] In contrast, the TrueBeam is equipped with a Millenium 120 leaf MLC. Furthermore, there are limited data on the new electron scattering foil geometries, and how this compares to other linear accelerators. Overall, there is a paucity of existing information in the literature on expectations related to the commissioning experience and expected nominal values for the TrueBeam geometry, particularly across multiple institutions with varied measurement practices.

Given the differences in MLC characteristics between the TrueBeam and TrueBeam STx, and the inherent differences between the other Varian machines (i.e., Trilogy), a summary of the mechanical and dosimetric properties of this new treatment unit is desirable. This work details the commissioning experience of five TrueBeam linacs, including timelines, baseline beam parameters, mechanical and multileaf collimator characteristics, end-to-end testing, and final dosimetric verification. The overarching goal of this work is to generate a set of data with technical guidelines that may assist other institutions embarking on TrueBeam commissioning, thereby improving the quality and safety of the commissioning process.

II. MATERIALS AND METHODS

Five TrueBeam linacs at three institutions were compared in this work: two at Henry Ford Health Systems (HFHS), two at University of Texas-Southwestern (UTSW), and one at University of Colorado-Denver (COL). At UTSW, two TrueBeam machines were considered "matched" with one mutual dataset for the two units along with spot checked data. Matching was performed by the physicists onsite after comparing machine acceptance and commissioning scans, photon and electron percent depth of ionization, and flatness and symmetry. For all five machines, the following photon energies were commissioned: 6X, 6XFFF, 10X, 10XFFF, and 15X. Electron energies of 6, 9, and 12 MeV were commissioned on all machines, with 16 and 20 MeV electron energies commissioned at two institutions and 15 and 18 MeV electron energies at the third. All five TrueBeams presented in this work were equipped with the 120 leaf Millenium MLC design, consisting of two opposing leaf banks with leaves that move along the X-axis. For the central 20 cm of the MLC, each leaf has a width of 5 mm projected at isocenter, whereas for the peripheral 10 cm on either side, the leaf width is increased to 10 mm.

Varian's Eclipse Treatment Planning System (Varian Medical Systems, Palo Alto, CA) was used to commission Anisotropic Analytical Algorithm (AAA) and Electron Monte Carlo (eMC) calculation models for photons and electrons, respectively, using the data collected. Table I outlines the estimated time required for each major acceptance and commissioning task based on all three institutions. Note that this makes the assumption that no major setbacks are encountered during the commissioning process.

For beam scanning, the Blue Phantom water tank (IBA Dosimetry GmbH, Germany), with scanning dimensions (i.e., servo range) of 48 × 48 × 48 cm, equipped with OmniPro Accept software (v. 6.5 or 7.2) was used. All beam scanning and data collection were performed in accordance with professional guidelines, such as AAPM Task Group (TG) Report Nos. 45 and 106,[2,3] providing detailed recommendations on acceptance testing, beam commissioning, proper measurement techniques, and detector selection—particularly for small field sizes.[4,5] Specific detector information for all institutions is shown in Table II. For field sizes $\leq 3 \times 3$ cm^2, small volume ion chambers or diodes were used per industry recommendations as outlined in Table II, and acquisition sampling time was increased to improve the signal to noise ratio.[3]

II.A. Isocenter verification

During machine acceptance, a Varian procedure for isocenter verification ("Isolock") was used to evaluate the central axis x-ray beam variation due to the gantry, couch, and collimator rotation.[6] Briefly, a collimated disk fixture is affixed to the gantry interface mount, projecting a circular field onto the MV imager. A tungsten BB, attached to a micrometer for fine positioning, is extended off the treatment couch and centered within the disk aperture at gantry angles of 0° and 90°. MV images were acquired using two different preprogrammed treatment plans: one at 63 different gantry/collimator angles and another with 13 different couch angles. Images were analyzed with proprietary software to verify that (1) the central axis x-ray beam variation due to the gantry and/or collimator positions was confined to a sphere of 0.5 mm radius, and (2) the central axis x-ray beam variation due to the gantry, couch, and/or collimator positions was confined to a sphere of 0.75 mm radius. Results from the Isolock tests were confirmed with an independent, EPID-based Winston Lutz (WL) test[7] to verify the isocenter stability was within a 1 mm tolerance. An example for HFHS included 12 portal images acquired at various gantry, couch, and collimator angles to assess isocenter movement. On each image, the difference between the center of a 2 × 2 cm^2, jaw-defined field and the center of the WL phantom (5 mm diameter, radio-opaque BB) was determined. Inplane deviations (ΔIP) and crossplane deviations (ΔCP) from radiation isocenter (shown in Fig. 1) were used to calculate the 3D offset of the BB location as well as the collimator and couch excursion during rotation. EPID images acquired at the four cardinal gantry angles were

TABLE I. Acceptance and commissioning timeline used for commissioning the Varian TrueBeam at three institutions.

Task	Estimated time commitment	Estimated FTE
Customer acceptance procedure of the linac and image guidance systems	2–3 weeks	1.0 physicist working with engineers
-Beam data acquisition (profiles, PDDs, factors: output, MLC transmission, leakage) -Preliminary TG-51 calibration -Independent TLD verification of linac calibration	4 weeks	2.0 physicists + 0.5 physicist for beam data processing for modeling
Beam modeling	1–2 weeks (offline)	1.0 physicist + 0.5 physicist for independent review of beam modeling process
-Misc. linac testing: isocentricity, MLC couch transmission -Misc. imaging testing: EPID, kV, and CBCT	2–3 weeks	2.0 physicists
-RapidArc commissioning -Collection of wedge factors and profiles for Enhanced Dynamic Wedge (including TPS verification)	1 week	2.0 physicists
-Verification measurements of TPS beam models -Verification of secondary independent dose calculation data and calculation (i.e., RadCalc)	1 week	1.0 physicist
Complete documentation of all acceptance/commissioning tasks	1 week	1.0 physicist
Routine monthly QA, including mechanical and output/calibration checks of the linac and QA of the image-guidance systems	Ongoing: 1.5–2 days (10–16 h)/month	1.0 Physicist
Patient-specific QA (plan preparation, delivery, analysis, and documentation)	Ongoing, patient load dependent: 1–2 h/patient	1.0 physicist
Routine annual QA including mechanical and output checks of the linac and QA of the image-guidance systems	Expected: 2 weeks (80 h)/year	1.0 physicist + 0.25 physicist for independent verification

analyzed to determine the 3D BB offset with respect to the radiation isocenter as follows:

$$(\mathrm{R}-/\mathrm{L}+) = (\Delta\mathrm{CP}, \mathrm{G0} - \Delta\mathrm{CP}, \mathrm{G180})/2,$$

$$(\mathrm{A}-/\mathrm{P}+) = (\Delta\mathrm{CP}, \mathrm{G90} - \Delta\mathrm{CP}, \mathrm{G270})/2,$$

$$(\mathrm{I}-/\mathrm{S}+) = (\Delta\mathrm{IP}, \mathrm{G0} + \Delta\mathrm{IP}, \mathrm{G90} + \Delta\mathrm{IP}, \mathrm{G180} + \Delta\mathrm{IP}, \mathrm{G270})/4.$$

The collimator and couch rotation excursions were defined as the 2D BB centroid distance $\sqrt{\Delta\mathrm{CP}^2 + \Delta\mathrm{IP}^2}$, from the center of the radiation field, averaged over all collimator and couch angles, respectively.

II.B. Photon characterization

II.B.1. Photon data acquisition

PDDs and profiles were taken in accordance with the Eclipse TPS algorithm manual. Field sizes ranged from 1 × 1 or 2 × 2 to 40 × 40 cm^2 and were determined by the jaw settings (i.e., data were acquired with the MLCs parked). All mandatory and recommended beam data measurements (PDDs, crossplane and inplane profiles) were performed, as specified in the Eclipse manual for commissioning AAA. The chamber position was automatically corrected for the effective point of measurement in the acquisition software.

II.B.2. Percent depth dose and profiles

Beam quality specifiers [i.e., $\mathrm{PDD}(10)_x$] were determined in accordance with TG-51.[8] PDD data at a variety of depths and field sizes were tabulated and compared among linacs. Penumbra was quantified and compared for all linacs for the transverse and radial beam profiles for 6X, 10X, and 15X beams. For FFF beams, however, the penumbra definition of the spatial distance between the 80% and 20% values does not apply, so the normalization technique introduced by Pönisch *et al.*[9] was employed. Briefly, penumbral widths were quantified after rescaling the FFF beam profiles to a ratio of the dose values at the inflection points in the penumbral regions between the unflattened and FFF beams, which has also been used in the literature.[1,10] In this work, we term this technique as "penumbra normalization." Data were also tabulated for polarity (P_{pol}) and ion collection efficiency (P_{ion}) for all photon energies using the two-voltage technique described in Task Group 51 using a setup of 100 cm SSD, 10 × 10 cm field size, at a chamber depth of 10 cm.[8]

TABLE II. Detectors used in multi-institutional TrueBeam commissioning study.

Type	Model	Sensitive volume	Diameter	Misc.	Institution	Tests performed
Cylindrical ion chambers	Scanditronix CC01	0.01 cm^3	2 mm	Steel central electrode	HFHS, COL	Electron OF and effective SSD (HFHS), photon FS 2×2^2 and 3×3^2 (COL photon OF and profiles $<3 \times 3^2$)
	Scanditronix CC13	0.13 cm^3	6 mm	C552 central electrode	HFHS, UTSW, COL	Photon profiles $\geq 4 \times 4$ cm^2 (UTSW and COL) photon OF (FS $\geq 4 \times 4$ cm^2) electron cone factors and PDDs
	Standard Imaging Exradin A12	0.65 cm^3	7.1 mm (outer shell)	C552 central electrode	HFHS	MLC transmission, DLG
	NE 2505/3A	0.6 cm^3	6.3 mm	Graphite wall, Al central electrode	COL	MLC transmission, DLG
	PTW 31014	0.015 cm^3	2 mm	Al central electrode; oriented in vertical direction	UTSW	Photon profiles $\leq 4 \times 4$ cm^2
	PTW 31013	0.3 cm^3	5.5 mm	Al central electrode, graphite coated	UTSW	MLC transmission, DLG, effective SSD
	PTW 30013	0.6 cm^3	5.5 mm	Al central electrode, graphite coated	UTSW	MLC transmission, DLG
Diode field detectors	Scanditronix PFD	0.12 mm^3	2 mm	Shielded	HFHS	Photon OF, $\leq 3 \times 3$ cm^2
	SunNuclear Edge Detector	0.0019 mm^3	Active detection area (mm): 0.8×0.8		UTSW	Photon OF $\leq 3 \times 3$ cm^2; photon profiles $\leq 2 \times 2$ cm^2
Detector array	IBA Linear Detector Array (LDA99)	2.0 mm diameter	5 mm spacing, 99 detectors	Hi-pSi diodes	UTSW	Wedge field profiles
	IBA Matrixx Planar Array	0.08 cm^3	7.62 mm spacing, 1020 detectors	Vented pixel ionization chambers	HFHS	Wedge field profiles, IMRT commissioning
	Sun Nuclear Profiler2	0.8 mm diameter	4 mm diode spacing, 139 detectors	Hi-pSi diodes	COL	Wedge field profiles

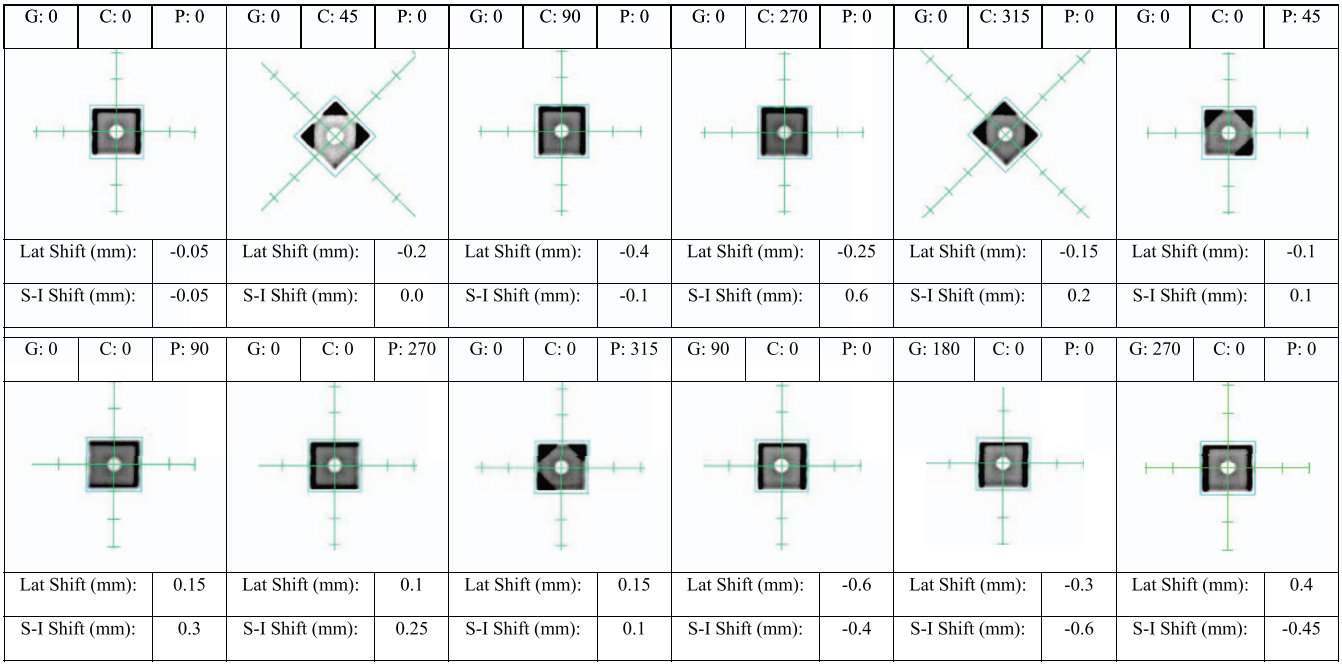

FIG. 1. Winston Lutz results obtained post-acceptance for a Varian TrueBeam as measured with the portal imager. A positive discrepancy in the crossplane direction indicates a shift to the right; a positive discrepancy in the inplane direction indicates an inferior shift. G = gantry angle, C = collimator angle, and P = pedestal angle.

II.B.3. Output factors (OFs)

For OF measurements, the field size was defined using the jaws. OFs were acquired using a CC13 cylindrical ion chamber for field sizes ranging from 3×3 cm^2 to the largest field size (30–40 cm on a side), and in all cases were normalized to a 10×10 cm^2 field size. One of the institutions measured OFs for slightly different field sizes, particularly for the range of 1×1 to 10×10 cm^2. When necessary, data were linearly interpolated between values to facilitate a more direct comparison. HFHS and UTSW acquired OFs at 100 cm SSD and 5 cm depth for all linacs, whereas COL acquired OFs at 100 cm SAD, 10 cm depth. To correct for this, tissue phantom ratios (TPRs), normalized to a depth of 10 cm were used to correct COL's output factors. Special consideration was given for small field dosimetry, as outlined in Sec. II.B.4.

II.B.4. Small field dosimetry

Small field dosimetry presents known challenges due to the interplay between the detector size/field dimension and the loss of lateral charged particle equilibrium.[4,5] For small field output factors, chamber selection and normalization methods were slightly different between institutions, although all followed current literature recommendations[3,4] and utilized a technique commonly referred to as "daisy chaining" that serves to correct energy dependence of different detectors.[11] At HFHS, a photon field diode (PFD) was used to acquire data field sizes $\leq 4 \times 4$ cm^2. An overlapping dataset was acquired using the CC13 chamber for fields 3×3 and 4×4 cm^2. A correction factor was applied to the 1×1 and 2×2 cm^2 field sizes by multiplying the average PFD reading at that field size by the following correction factor: OF CC13(4×4 cm^2)/PFD(4×4 cm^2). Similar techniques were followed by UTSW (diode detector used for 2×2 and 3×3 cm^2, CC13 for field sizes $\geq 3 \times 3$ cm^2) with a correction factor derived for the 2×2 cm^2 field based on the overlapping 3×3 cm^2 dataset. Similar methods were used at COL, although a CC01 chamber and 4×4 cm^2 reference field were employed.

II.B.5. Leaf transmission and dosimetric leaf gap (DLG) measurements

MLC transmission was measured separately for both MLC leaf banks, with the rounded MLC leaf tips abutted underneath the jaws to minimize the effects of intra- and interleaf leakage in the transmission measurement. For four TrueBeam linacs, a Farmer-type chamber (collecting volume $= 0.65$ cm^3) was used, and for the other (HFHS2), a CC13 was employed. The setup was the same for both HFHS linacs and COL (90 cm SSD, 10 cm depth), although UTSW used a 100 cm SSD at a 10 cm depth. All measurements were performed in water, with jaw sizes set to 10×20 cm, using DICOM plans provided by Varian.[12] For each energy, average transmission readings were calculated by averaging the results for each MLC bank. According to TG-50, the average leaf transmission should be $<2\%$.[13]

Using the same setup as for leaf transmission, the DLG—or the factor used to account for the transmission through rounded leaf edges—was measured for all photon energies using a technique and DICOM plan files provided by the manufacturer.[14] Charge readings were measured for a variety of sliding MLC gap widths (1, 2, 4, 6, 10, 14, and 20 mm) spanning 120 mm at a constant speed. The contribution of the average MLC leaf transmission was accounted for, and a plot was generated of the corrected gap reading versus the gap size. A linear fit was performed, and the Y-intercept indicated the DLG (in mm).

II.B.6. IMRT commissioning

At HFHS, IMRT commissioning was performed in accordance with TG-119 recommendations with an emphasis on the higher complexity plans provided by this Task Group[15] for both TrueBeams commissioned. Verification of plan delivery involved point and planar dose measurements delivered at the actual gantry angles using the CC01 chamber listed in Table II and GAFCHROMIC™ EBT2 film (International Specialty Products, Wayne, NJ), respectively. Gafchromic film processing and subsequent gamma analysis was performed using a scan and transpose technique.[16] Briefly, two sets of films (calibration and treatment plan films) are irradiated in a slab phantom with one film flipped left-right to compensate for nonuniform film response. After ~12 h postirradiation, each film was scanned in four different orientations to mitigate nonuniform response of the scanner light and detector elements. The scanned eight calibration and eight plan images were averaged into one calibration and one plan film image, respectively. Each color channel of the calibration film was correlated to the reference dose matrix to produce a third order polynomial calibration curve. Finally, each color channel of the plan film was converted to a dose map using the corresponding calibration curve. Average dose maps of the red and green channels were correlated to the treatment planning dose matrix for subsequent analysis.

A TG-119 nine-field IMRT treatment plan using 6XFFF consisting of a C-shape target (i.e., PTV) that surrounds a central core avoidance [i.e., organ at risk (OAR)] structure of 1 cm radius was delivered. This plan was the most challenging, where the central core was to receive $<20\%$ of the target dose. Point dose measurements were conducted in both low and high dose regions, in the central core and in the middle of the PTV (2.5 cm anterior to isocenter), respectively. TG-119 plans were also calculated and delivered using a RapidArc delivery technique. Composite point dose differences were characterized as defined by TG-119: [(measured dose − plan dose)/prescription dose]. Note that this is a unitless quantity. Results from HFHS TrueBeam 1 and 2 are presented.

II.C. Electron characterization

All TrueBeam machines studied shared electron energies of 6, 9, and 12 MeV. For high energy electrons, three linacs

had 16 and 20 MeV, while UTSW commissioned 15 and 18 MeV for their two linacs. All mandatory and recommended beam data measurements according to the Eclipse algorithm manual (PDDs, crossplane and inplane profiles) were performed for all available energies using a CC13 chamber at all institutions. Electron cone sizes ranged from 6×6 to 25×25 cm^2 using standard cutouts. Beam quality specifiers were determined as defined by TG-51 (i.e., R_{50}, a quantity calculated from 50% of the maximum ionization value on the depth-ionization curve).[8] Electrons were also characterized via other commonly used parameters including practical range (R_p), the depth of 90% dose level (often defined as the therapeutic range) (R_{90}), depth of maximum dose (D_{max}), and the most probable energy (E_p).[17]

II.C.1. Electron cone factors

At all three institutions, electron cone factors were measured using the CC13 chamber positioned at D_{max}, 100 cm SSD, and for the purpose of this paper, were normalized to the 15×15 cm^2 electron cone. Mean, standard deviation (SD), and coefficient of variation (defined as the ratio of standard deviation to the mean) were computed for each cone factor for the following: 6, 9, and 12 MeV for 5 linacs, and 16 and 20 MeV for 3 linacs.

II.C.2. Effective SSD

For two institutions, the effective SSD was determined by taking measurements at each energy's D_{max} at varied air gaps between the electron cone and water surface, plotting the square root of I_0/I and the gap distance (ranging from 0 to 15 cm), and determining the linear fit as outlined by Khan.[18] Data were acquired for cone sizes 6×6 through 25×25 for all electron energies using standard cutouts. Note that at higher electron energies, UTSW included 15 and 18 MeV, whereas the HFHS TrueBeams had 16 and 20 MeV. Here, HFHS used a CC01 detector, whereas UTSW used a PTW 0.3 cc detector. Clinical practice at COL involves measuring cutout factors on an as-needed basis if the treatment is not at standard 100 cm SSD, and therefore comparison data were not generated for this institution.

II.D. Other characteristics

II.D.1. Couch transmission

The IGRT couchtop consists of two main sections: a 7.5 cm thick portion (water equivalence of 8.5 mm at 6 MV), and a 5 cm thin portion (water equivalence of 5.2 mm at 6 MV). The outer shell is made of carbon fiber, while the interior consists of a lightweight foam core. Couch transmission measurements were performed in solid water with the detector placed at isocenter for all photon energies. First, 100 MU were delivered using a 10×10 cm^2 field size with no couch perturbance. Then, measurements (100 MU) were made with the thick and thin portions, as defined above, of the couch positioned over the chamber location. Percent transmission was defined as the ratio of charge measured with the couch divided by the charge measured without the couch in place and converted to a percentage.

II.D.2. End-to-end testing

End-to-end tests, including CT simulation, treatment planning, localization, and dosimetric verification, were performed to assess the overall accuracy of each TrueBeam commissioned. For HFHS1, the Lucy 3D QA Phantom (Standard Imaging, Middleton, WI) designed for stereotactic QA with MRI Isocentric Volume insert coupled with dosimetry analysis was used as described previously.[19] Briefly, 2 mm CT slices of the Lucy phantom were acquired, a central contour (irregular region of interest created by mineral oil) was delineated, and isocenter was set to the centroid of the contour. Data were exported to treatment planning, and two plans were generated: a single arc RapidArc, and a nine-field IMRT plan. Data were transferred to the TrueBeam, MV/KV images were used for localization, and the plans were delivered to a PTW PinPoint chamber for point dose measurement. A similar process was also followed for HFHS2. Here, the Rando thorax phantom with an implanted BB went through the CT-simulation process, a treatment plan (nine IMRT fields using the BB as the isocenter) was derived following RTOG 0915 criteria,[20] and Gafchromic film analysis was performed for a nearby axial plane using the film dosimetry process described in Sec. II.B.6. The plan was transferred to the TrueBeam where the phantom was set up to external marks using the lasers, initial BB localization was performed with a CBCT, and then residual error was quantified via verification images consisting of CBCT, an orthogonal KV set, and an orthogonal MV set.

UTSW performed the IMRT head and neck credentialing test through the RPC for their end-to-end testing.[21] The RPC anthropomorphic head phantom includes TLD capsules to assess point doses in PTV and OAR regions, as well as GAFChromic film at the center of the PTV to assess dose profiles. A planning CT scan was acquired, an IMRT plan was constructed, and the phantom was localized using IGRT and subsequently irradiated. Independent peer review was also performed via the RPC for independent dosimetric validation (optically stimulated luminescence detectors for each energy) (results not shown).

II.D.3. Temporal stability

Output factors were reported for all five linacs for 6, 10, and 15 MV photons, and 6, 9, and 12 MeV electrons at monthly intervals from the commissioning date (5–8 months of data/machine). 6XFFF and 10XFFF were not in clinical use at UTSW due to compatibility issues with the record and verify system, so they were omitted from the analysis. Two of the institutions measured monthly output in a small water tank, while the third used solid water coupled with a Farmer chamber.

III. RESULTS

III.A. Isocentricity

Gantry/collimator isocentricity ranged from 0.265 to 0.283 mm for all linacs, which were well within the Varian specification of a 0.5 mm radius. Larger variations were observed for the couch/gantry/collimator isocenter axis where radii ranged from 0.464 to 0.675 mm across the institutions, which was still within the Varian specification (0.75 mm radius). An example of an independent Winston Lutz test acquired with the EPID imager is shown in Fig. 1. Quantitative analysis determined a 3D BB offset of 0.13, −0.50, and −0.38 mm in the lateral, anterior-posterior, and superior-inferior dimensions. The average collimator and couch rotation excursions were 0.32 ± 0.22 and 0.20 ± 0.10 mm, respectively. These deviations are well within the 1 mm tolerance, as expected based on our Isolock results.

III.B. Photon measurements

III.B.1. Depth dose and profile agreement

Table III best summarizes photon metrics studied. For 6, 10, and 15 MV photon beam quality, %dd(10) varied less than 0.3% for all machines. The largest deviations in percent depth doses between institutions occurred for the 30 × 30 cm^2 field sizes at 20 cm depths. Figure 2 shows the close agreement obtained for 10XFFF and 15X at both 10 × 10 and 40 × 40 cm^2. P_{ion} values were slightly higher for the FFF modes than their flattened counterparts, while P_{pol} yielded similar values for all energies. Close agreement in P_{ion} and P_{pol} was observed for all TrueBeam machines measured.

Penumbra measurements agreed well for 6X, 10X, and 15X (standard deviations of the mean values <0.5 mm). For all energies, inplane penumbra values were larger than crossplane. For FFF modes, the "penumbra normalization" method was employed, and this technique revealed a discrepancy for COL's 6XFFF 30 × 30 cm^2 cross and inplane penumbra calculations that deviated from other machines by ∼2.5 and ∼5 mm, respectively. Despite this calculated discrepancy, Fig. 2 shows close agreement between inplane and crossplane profiles for all TrueBeam linacs for both 6XFFF and 10XFFF, with the exception of the increased low dose tails near ∼20 cm from central axis (CAX) for COL. The profiles for all tails at ∼20 cm from CAX were elevated for all COL data, including the flattened beams (not shown). It was discovered that when the Wellhofer Blue Phantom2 system, with coupled controller and two integrated electrometers, was placed inside the linac vault on the treatment table, scatter from the water tank biased the electrometer readings, thus, contributing to higher out of field readings. PDDs were remeasured once this was discovered, although the profiles were deemed acceptable in the clinically relevant regions. Because of the interference from the controller and its impact on the 6XFFF, 30 × 30 cm^2 field size, COL was omitted from the mean and standard deviation calculations for both inplane and crossplane profile penumbras, as stated in Table III.

III.B.2. Leaf transmission and dosimetric leaf gap measurements

Table IV summarizes the available data for the DLG and MLC transmission for all photon energies. For HFHS2 and COL, measured DLG values were optimized to fit Eclipse dose calculations to measurements, in a manner similar to Chauvet *et al.*[22] These optimized parameters are reflected in the table for the two machines. HFHS1 measured DLGs were, on average, ∼0.4 mm less than the other two institutions for all energies, despite using the same measurement technique (vendor-supplied DICOM files and experimental setup). The overall standard deviations of the DLGs were less than 0.3 mm for all energies. MLC transmission showed minimal variation across the three institutions. The largest MLC transmission values were observed for 10X for all institutions.

III.B.3. Output factors

After correcting for differences in OF setup conditions, minimal variation was observed among relative photon output factors. Figure 3 demonstrates the photon output factors for field sizes ranging from 4 × 4 to 40 × 40 cm^2 as

TABLE III. Photon beam parameters. Average data ± standard deviation summarized for three institutions (five TrueBeam linear accelerators). All parameters showed close agreement except as noted below. Penumbra values shown were taken at a depth of 10 cm using CC13 chambers. Field sizes 10 × 10 and 30 × 30 cm^2 are tabulated.

			Photon percent dose (%) Mean ± StDev						Penumbra (mm) Mean ± StDev			
Energy			5 cm		10 cm		20 cm		Transverse (crossplane)		Radial (inplane)	
(MV)	P_{pol}	P_{ion}	10 × 10	30 × 30	10 × 10	30 × 30	10 × 10	30 × 30	10 × 10	30 × 30	10 × 10	30 × 30
6X	0.999±0.002	1.003±0.002	85.8±0.2	87.6±0.3	66.2±0.3	70.6±0.6	38.1±0.3	44.3±1.0	6.82±0.13	9.02±0.42	7.67±0.15	10.06±0.42
10X	0.999±0.002	1.004±0.001	91.5±0.1	91.4±0.1	73.5±0.1	75.7±0.4	46.4±0.2	50.6±0.7	7.42±0.08	9.06±0.15	8.36±0.20	10.05±0.27
15X	0.998±0.002	1.005±0.001	94.1±0.2	91.8±0.2	76.6±0.1	76.6±0.3	49.9±0.2	52.4±0.6	7.56±0.06	8.98±0.15	8.13±0.11	9.62±0.26
6XFFF	0.999±0.001	1.006±0.002	84.3±0.2	86.3±0.2	63.3±0.1	67.5±0.3	34.5±0.2	39.9±0.4	6.96±0.22	9.49±0.21[a]	7.65±0.51	10.39±0.82[a]
10XFFF	0.999±0.001	1.010±0.004	90.4±0.1	90.9±0.1	71.0±0.1	73.0±0.1	42.9±0.1	46.2±0.3	6.98±0.12	8.89±0.59	8.08±0.43	9.65±0.57

[a]COL inplane and crossplane penumbra data for 6XFFF, 30 × 30 cm^2 was omitted. See text for full description.

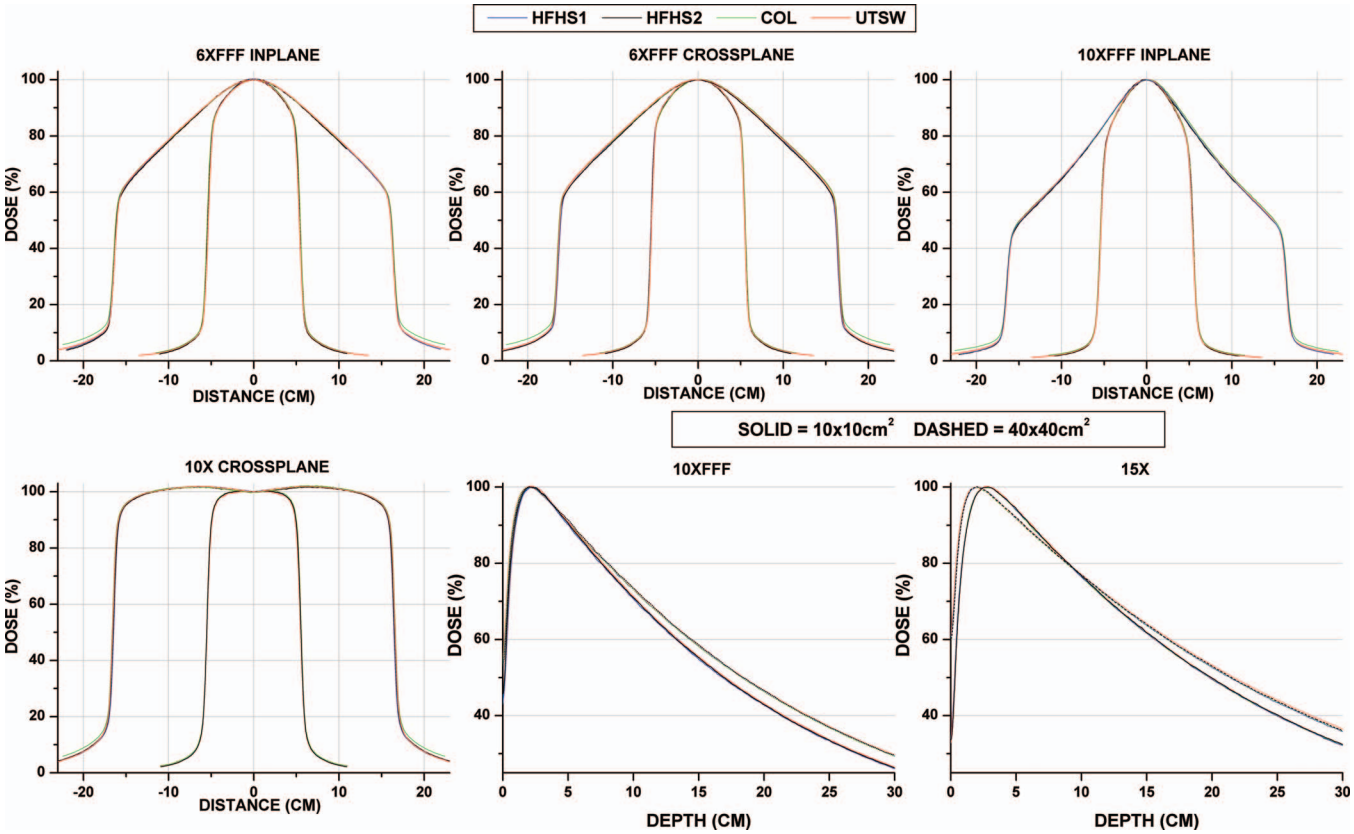

FIG. 2. Inplane and crossplane profiles for 6XFFF and 10XFFF for different TrueBeam linear accelerators (10×10 and 30×30 cm^2 field sizes shown). Data were well-matched except for one institution in the low dose tail region. PDDs for all photon energies also demonstrated good agreement (10XFFF and 15X shown for both 10×10 and 40×40 cm^2).

measured with a CC13 chamber. Excellent agreement was found among all output factors; the largest coefficient of variation was 0.5% for the 40×40 cm^2 field at 6X. Small field output factors are shown in Fig. 4 to better enhance small differences in the deviations between machines. The maximum standard deviation for all output factors studied was 0.01 for the 10X, 2×2 cm^2 field size (1.18% coefficient of variation). The average coefficient of variation for all output factors studied was 0.28%.

III.B.4. IMRT commissioning

Composite Gafchromic film results from TG-119 are shown in Fig. 5 for the "CShape-Hard" plan at the central core level for HFHS1. The percentage of points passing the recommended 3%/3 mm Gamma criteria was 99% for both the low and high dose planes. Using the TG-119 definition of dose difference ratios (i.e., expressed as a ratio of prescription dose), a composite point dose differences of 0.0056 (3.3 cGy difference) and 0.0088 (5.3 cGy difference) were measured for the central core and high dose regions, respectively, at a prescription dose of 600 cGy. For HFHS2, slightly better agreement between the planned and measured dose differences were obtained [TG-119 dose difference ratios were 0.000 (0.001 cGy difference) and 0.004 (0.007 cGy difference) for the central core and high dose regions, respectively, at a prescription dose of 200 cGy].

A single arc RapidArc plan was also devised for the same "CShape-Hard" plan, and the TG-119 defined dose difference

TABLE IV. Miscellaneous commissioning values for all photon energies combined. All data summarized for three institutions (five TrueBeam linear accelerators).

	Dosimetric leaf gap Mean ± StDev (mm)	MLC transmission Mean ± StDev (%)	Thin couch transmission Mean ± StDev (%)	Thick couch transmission Mean ± StDev (%)
6X FFF	1.16 ± 0.22	1.36 ± 0.11	97.26 ± 0.21	96.33 ± 0.40
6X	1.33 ± 0.23	1.58 ± 0.07	97.60 ± 0.24	96.84 ± 0.47
10X FFF	1.44 ± 0.30	1.63 ± 0.10	98.01 ± 0.11	97.22 ± 0.21
10X	1.57 ± 0.24	1.79 ± 0.04	98.17 ± 0.26	97.57 ± 0.35
15X	1.61 ± 0.26	1.74 ± 0.03	98.44 ± 0.05	97.85 ± 0.28

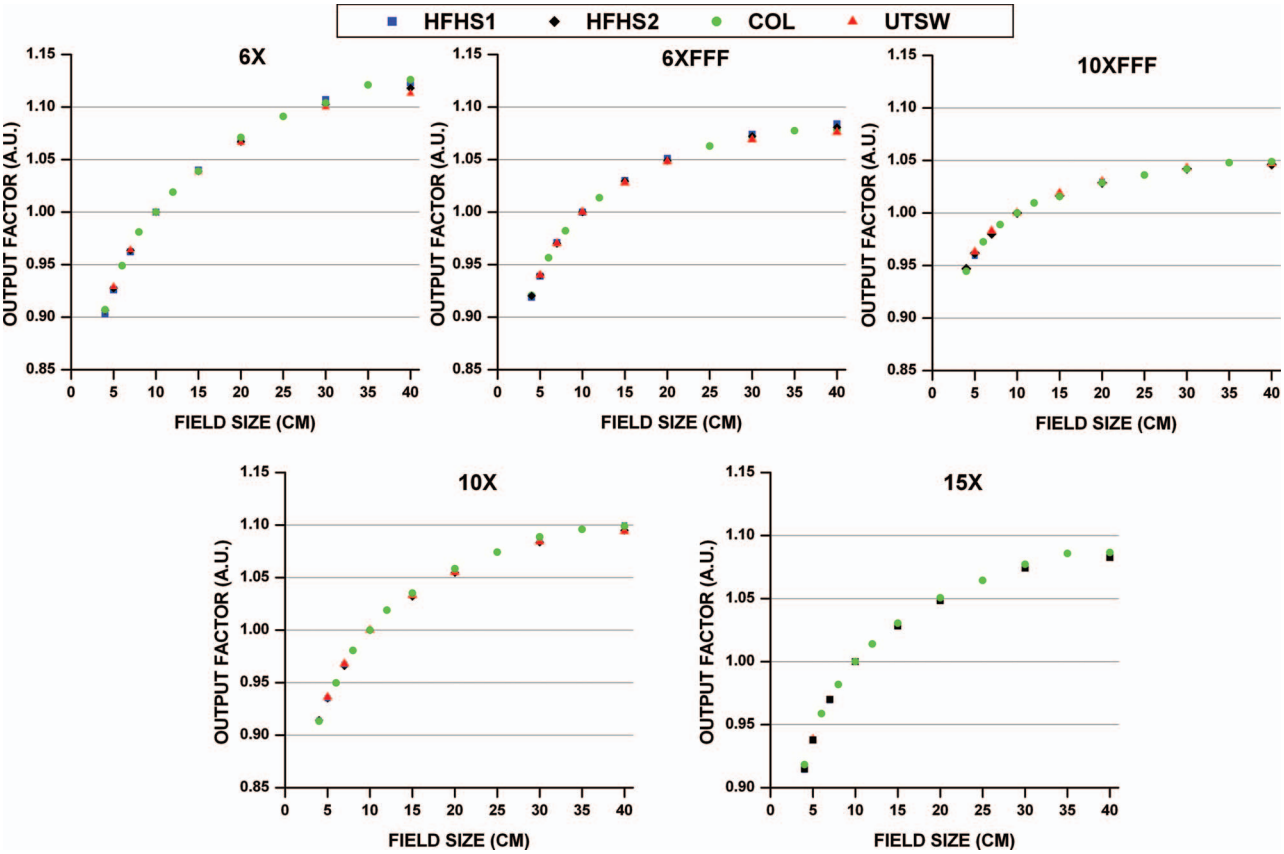

FIG. 3. Photon output factors for five TrueBeam linear accelerators measured at three institutions. Excellent agreement was found among all output factors; the largest coefficient of variation for all output factors greater than 4×4 cm^2 was 0.5% for the 40×40 cm^2 field at 6X.

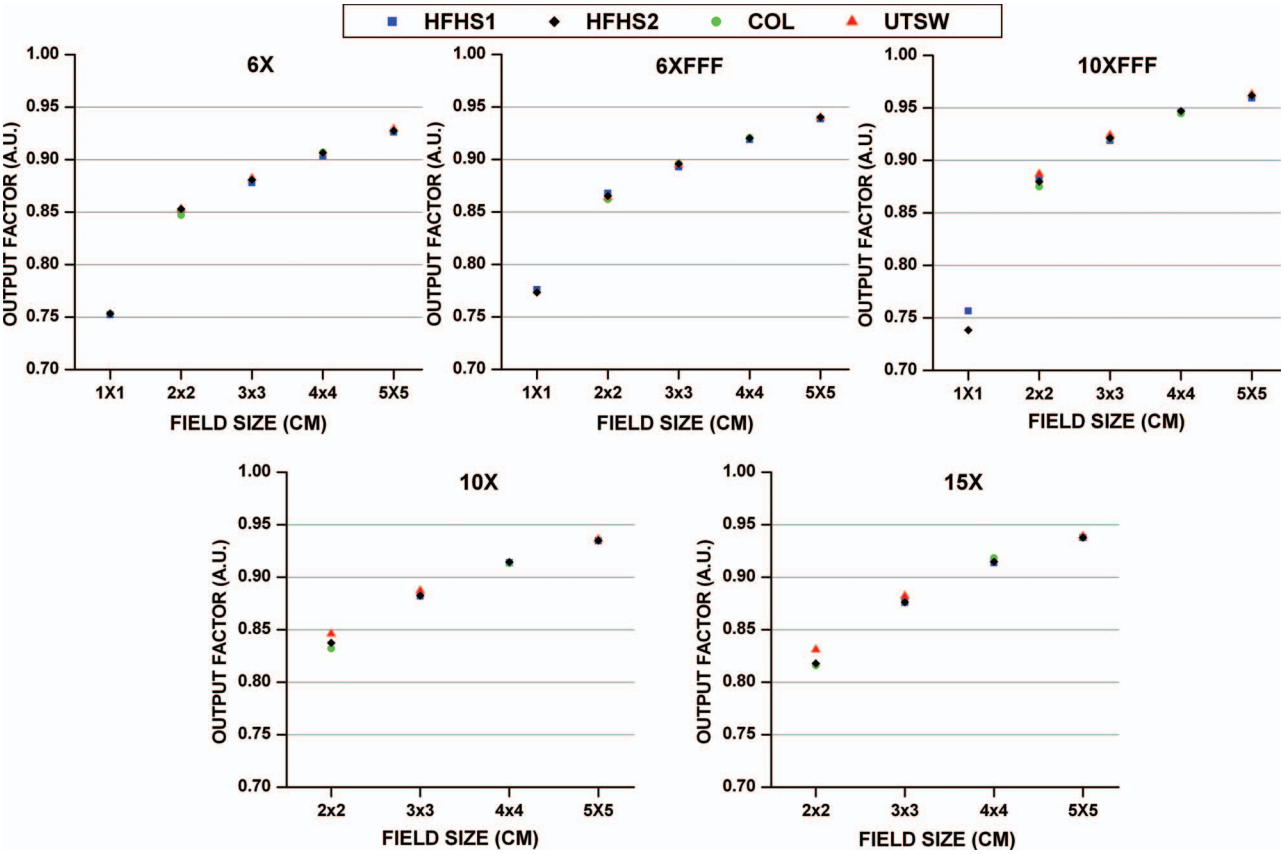

FIG. 4. Small field output factors for all photon energies for five TrueBeam linear accelerators.

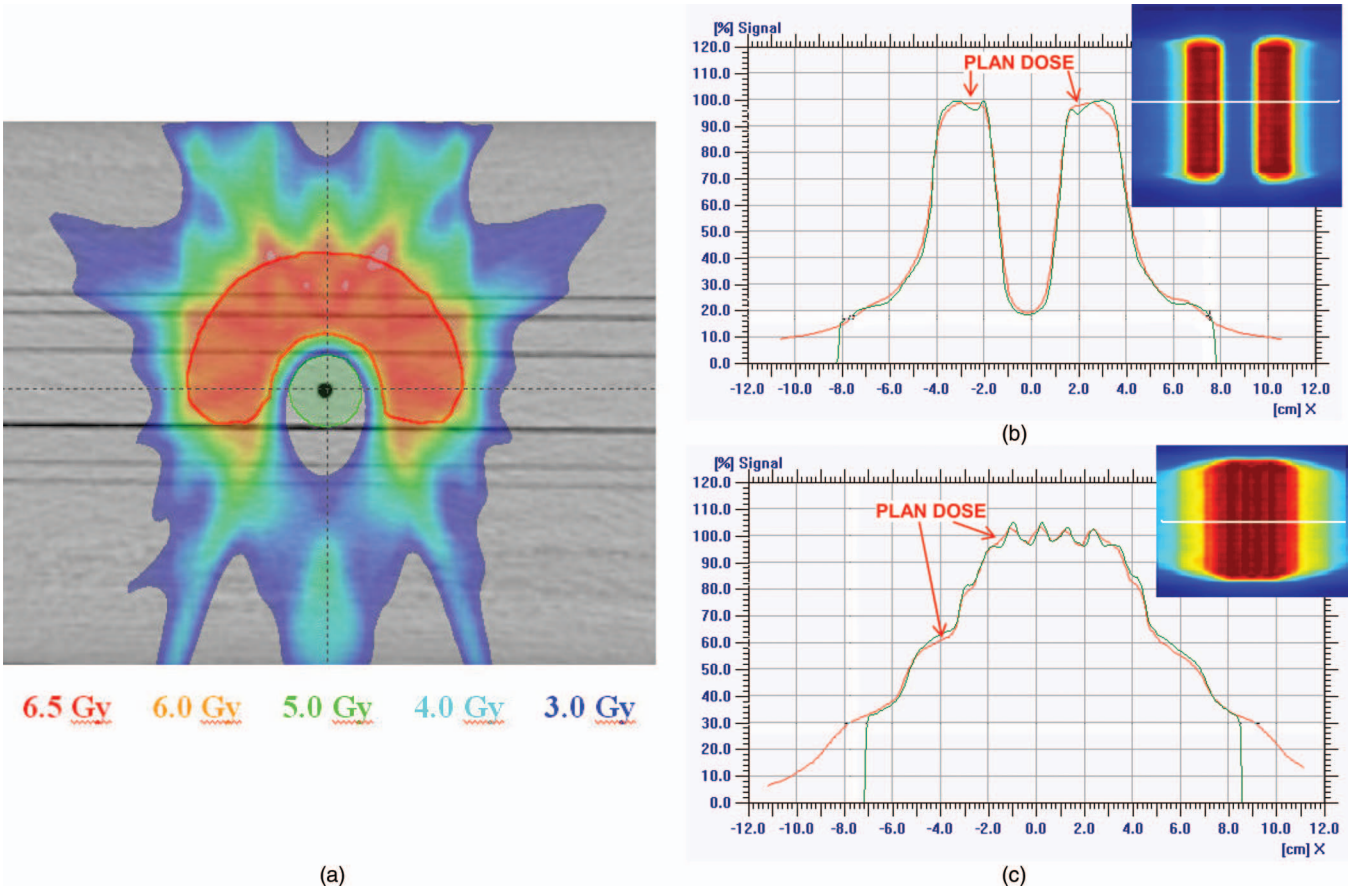

FIG. 5. (a) Planned axial dose distribution at central core level (i.e., low dose region) of 6XFFF Hard C-Shape plan from the TG-119 test suite demonstrating the C-Shape PTV with nearby cylindrical shaped organ at risk. (b) Gafchromic film measurement results for the lateral (x-y) profile comparing the planned versus measured fluence in (b) low dose (level of core) and (c) high dose (level of PTV) regions. For (b) and (c), the labeled line indicates the planned dose, whereas the truncated profile in the X-direction indicates the measured dose profile.

ratio was 0.0128 (7.7 cGy difference) and 0.0121 (7.2 cGy difference) for the central core (low dose) and high dose regions, respectively. For HFHS2, the same plan yielded TG-119 results of 0.016 and 0.023 for the central core (low dose) and high dose regions, respectively. Here, point dose chamber results were 7.3% and 1.1% different for the central core and high dose regions, respectively, for HFHS1, which were similar to those obtained for HFHS2 (6.7% and 2.2% different than expected for the same regions).

III.C. Electron characterization

PDD parameters for all electron energies studied demonstrated excellent agreement, with <1 mm standard deviation of the mean for all parameters evaluated (Table V). The electron beam quality specifier (R_{50}) showed overall good agreement between machines, with the largest difference occurring at 12 MeV (1.5 mm range across four TrueBeam machines).

III.C.1. Electron cone factors

Electron cone factors were well matched for all energies and field sizes, as shown in Fig. 6. The largest discrepancy across all machines was observed for the 12 MeV, 6 × 6 cm electron cone (maximum standard deviation = 0.0083 arbitrary units, CV = 0.87%). Over all electron cones and energies, the average CV was 0.23 ± 0.25%.

III.C.2. Effective SSD

Figure 7 demonstrates effective SSD measurements for UTSW and two HFHS TrueBeam machines. Overall, close agreement was observed between the HFHS machines for all energies. UTSWs measured effective SSD tended to be lower in magnitude for 6, 9, and 12 MeV compared to the other two units, although the same general trends were observed. The largest variation between all machines was observed for the 6 × 6 cm electron cone, particularly at lower energies (i.e., 6 MeV). Here, UTSW was ~3–4 cm shallower than the HFHS measured machines.

III.D. Evaluation of other characteristics

III.D.1. Couch transmission

Table IV summarizes couch transmission results for the thick and thin portions of the Varian IGRT Couch for all photon energies.

TABLE V. Electron beam mean and standard deviation (STD) parameters for three institutions for the 20 × 20 cm electron cone.

	D_{max} (cm)	R50 (cm)	R90 (cm)	Rp (cm)	Ep (MeV)
			6 MeV		
HFHS1	1.26	2.33	1.72	3.00	6.19
HFHS2	1.20	2.29	1.69	2.91	6.00
COL	1.26	2.41	1.79	3.07	6.32
UTSW	1.25	2.37	1.75	3.05	6.29
Mean	1.24	2.35	1.74	3.01	6.20
SD	0.03	0.05	0.04	0.07	0.14
			9 MeV		
HFHS1	1.98	3.50	2.67	4.37	8.91
HFHS2	2.00	3.50	2.68	4.35	8.87
COL	2.07	3.61	2.77	4.49	9.16
UTSW	2.08	3.63	2.78	4.50	9.19
Mean	2.03	3.56	2.73	4.43	9.03
SD	0.05	0.07	0.06	0.08	0.17
			12 MeV		
HFHS1	2.80	4.93	3.82	6.05	12.29
HFHS2	2.76	4.96	3.82	6.04	12.28
COL	2.82	5.01	3.89	6.15	12.50
UTSW	2.78	5.08	3.94	6.21	12.60
Mean	2.79	5.00	3.87	6.11	12.42
SD	0.03	0.07	0.06	0.08	0.16
			16 MeV		
HFHS1	2.90	6.57	4.99	8.08	16.38
HFHS2	2.85	6.58	5.04	7.94	16.10
COL	2.97	6.65	5.07	8.10	16.43
Mean	2.91	6.60	5.03	8.04	16.30
SD	0.06	0.04	0.04	0.09	0.18
			20 MeV		
HFHS1	2.35	8.23	5.97	10.17	20.61
HFHS2	2.5	8.22	6	10.05	20.38
COL	2.47	8.27	6.00	10.11	20.49
Mean	2.44	8.24	5.99	10.11	20.49
SD	0.08	0.03	0.02	0.06	0.12

III.D.2. End-to-end testing

For end-to-end testing for HFHS1, after localizing the Lucy phantom scribes to the lasers, <0.5 mm in the vertical, longitudinal, and lateral directions were needed for proper isocenter alignment using an MV/KV orthogonal pair. The nine-field IMRT plan demonstrated a 0.4% difference in overall point dose between the planned and measured values (per beam range: −0.60% to 1.20%) and the single arc RapidArc plan was −0.23% different from expected.

For HFHS2, initial CBCT localization of the BB implanted in the Rando thorax phantom was −0.8, 0.9, and 1.3 mm different from external laser alignment in the vertical, longitudinal, and lateral directions, respectively. Residual error analysis showed 0 mm discrepancy in the vertical and longitudinal directions using three imaging modalities (CBCT, KV/KV, and MV/MV orthogonal sets), although the lateral direction showed a slight residual discrepancy for all imaging modalities (0.2–0.3 mm). Gamma analysis of Gafchromic EBT3 film dosimetry in the axial plane revealed 99.8% of pixels passed within scribed region at a 3%/3 mm distance to agreement, and 94.7% pass rate using 2%/2 mm criteria as shown in Fig. 8.

UTSW passed the head and neck RPC IMRT credentialing test. In the target (PTV) region, point doses measured by TLDs had measured/institution ratios of 0.94–0.99 (RPC acceptable criteria = 0.93–1.07). The organ at risk was assessed via film profiles scaled to TLD dose values. Isodose lines (mean of three levels) from institutional treatment plans were used to measure the displacement between the measured and expected dose gradients in the region between the PTV and the OAR, with a 4 mm tolerance. This difference was calculated to be 0 mm.

III.D.3. Temporal stability

Figure 9 demonstrates monthly central axis output measurements for all photon energies available on the TrueBeam units. As mentioned previously, flattening filter free modes were not compatible with the record and verify system at UTSW and were therefore unavailable for comparison. Electron energies followed similar patterns as the photons (data not shown). Output was reduced at months 3 and 6 for all energies at HFHS due to observed upward trends and an institutional limit of 1.5% of nominal calibration. Output was also reduced at month 6 at COL, and at months 4 and 7 for UTSW Machine 2.

IV. DISCUSSION

This study summarizes the commissioning experiences of five TrueBeam linear accelerators at three different institutions, including timelines, mechanical, and dosimetric parameters. Table I demonstrates the timelines and personnel required for commissioning and ongoing QA efforts, which are slightly increased compared to standard linear accelerators due to the extra photon modes available for the TrueBeam. However, when compared to the expected commissioning and QA effort for a NovalisTX that includes both OBI and ExacTrac imaging systems, as well as Eclipse and iPlan Treatment Planning system, the overall effort was similar.[19] Overall, TrueBeam parameters demonstrated excellent agreement across all machines. For example, MLC transmission showed minimal variation across the five machines, with the standard deviation <0.2% for all linacs studied. The largest transmission values were observed for 10X for all machines. This is expected, as the increased pair production at 15X results in lower overall transmission than at 10X. The relative photon output factors were also in excellent agreement (largest standard deviation for all output factors was 0.01 for a 2 × 2 cm^2 field at 15X, corresponding coefficient of variation of 1.2%). For field sizes >10 × 10 cm^2, the output factors for the FFF modes tended have a smaller magnitude than their flattened counterparts (i.e., 6XFFF and 6X, 10XFFF and 10X), which is consistent with the literature.[1]

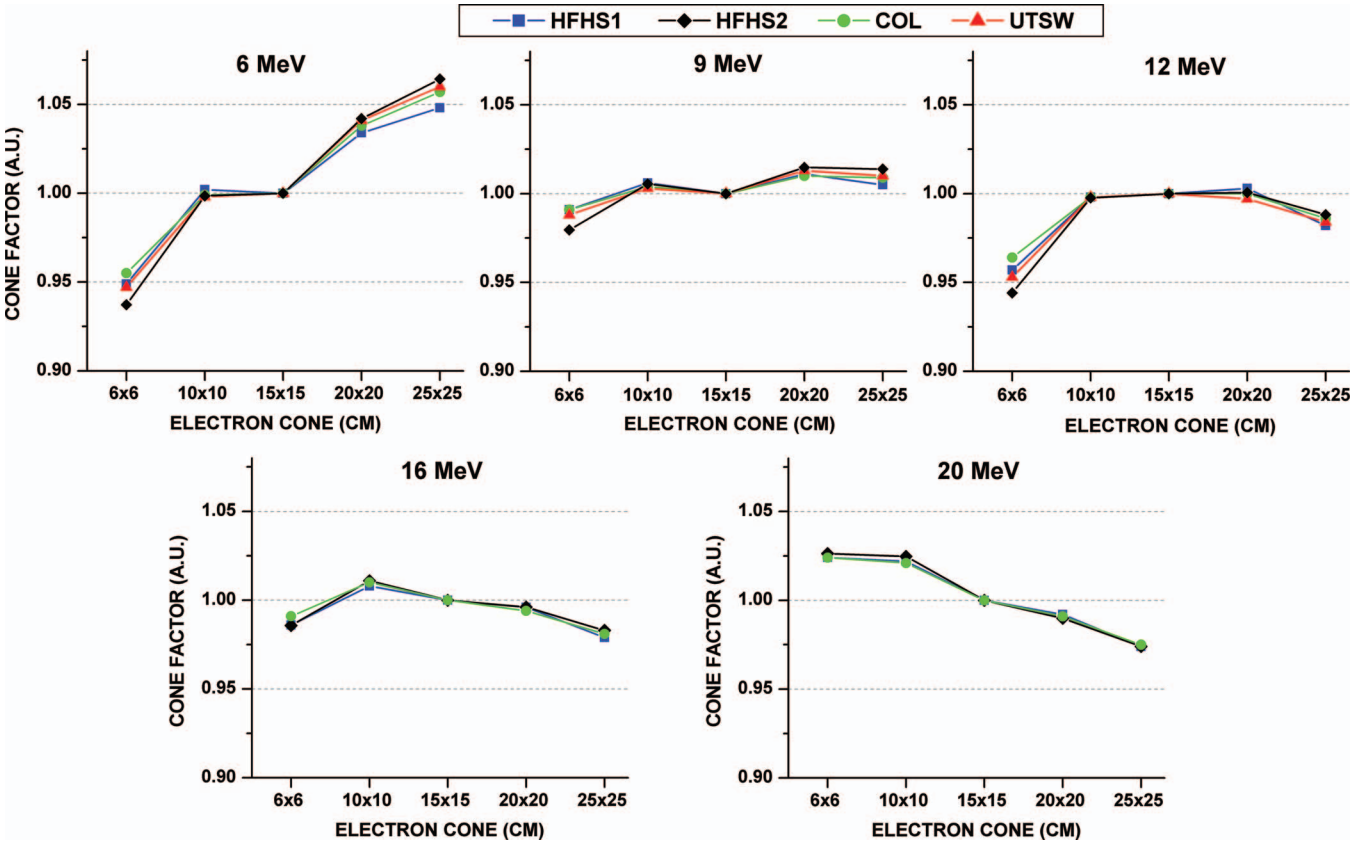

FIG. 6. Electron cone factors for 6, 9, and 12 MeV for all five TrueBeam linear accelerators, with UTSW data representing two matched machines. 16 and 20 MeV data shown for three TrueBeam linear accelerators with mutual high energies.

PDDs shown in Fig. 2 demonstrated close agreement for the 10XFFF and 15 MV photons. Inplane/crossplane profiles for FFF modes were well matched between machines, with the exception of the low-dose tails for COL as described in Sec. III. Over all energies studied, inplane penumbra values were slightly larger than crossplane, which is consistent with the literature.[23] Despite being well matched among institutions, average measured penumbra values for 6, 10, and 15 MV beam energies were slightly larger (~1–2 mm) than what have been reported for two other analyses of TrueBeam machines.[23,24] The likely cause of this discrepancy is the selection of ionization chamber that was employed for measurements, as Chang *et al.*[23] used a combination of high-resolution diode detectors (i.e., stereotactic field detector) and ion chambers (CC01 and CC13) to measure their dosimetric data. High resolution diodes and chambers are desirable to describe penumbra regions, which was performed for all small field dosimetry in this work. Overall, close agreement in polarity and ion collection efficiency was observed for all photon energies studied. P_{ion} values were slightly higher for the FFF modes than their flattened counterparts, with 10XFFF yielding the largest correction (1.010 ± 0.004

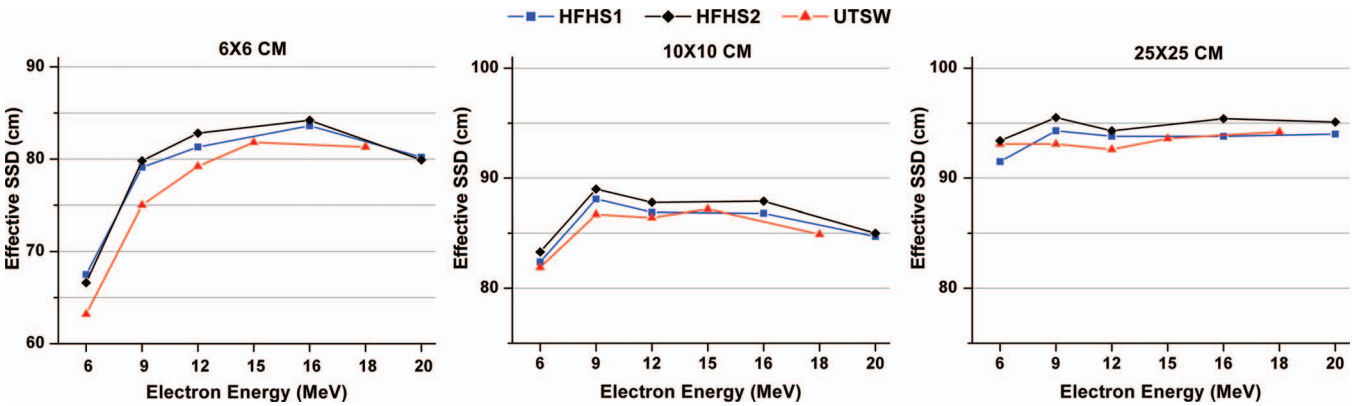

FIG. 7. Effective SSD results for two institutions, four linacs with new scattering foil geometries for the TrueBeam. UTSW represents a single dataset for matched machines.

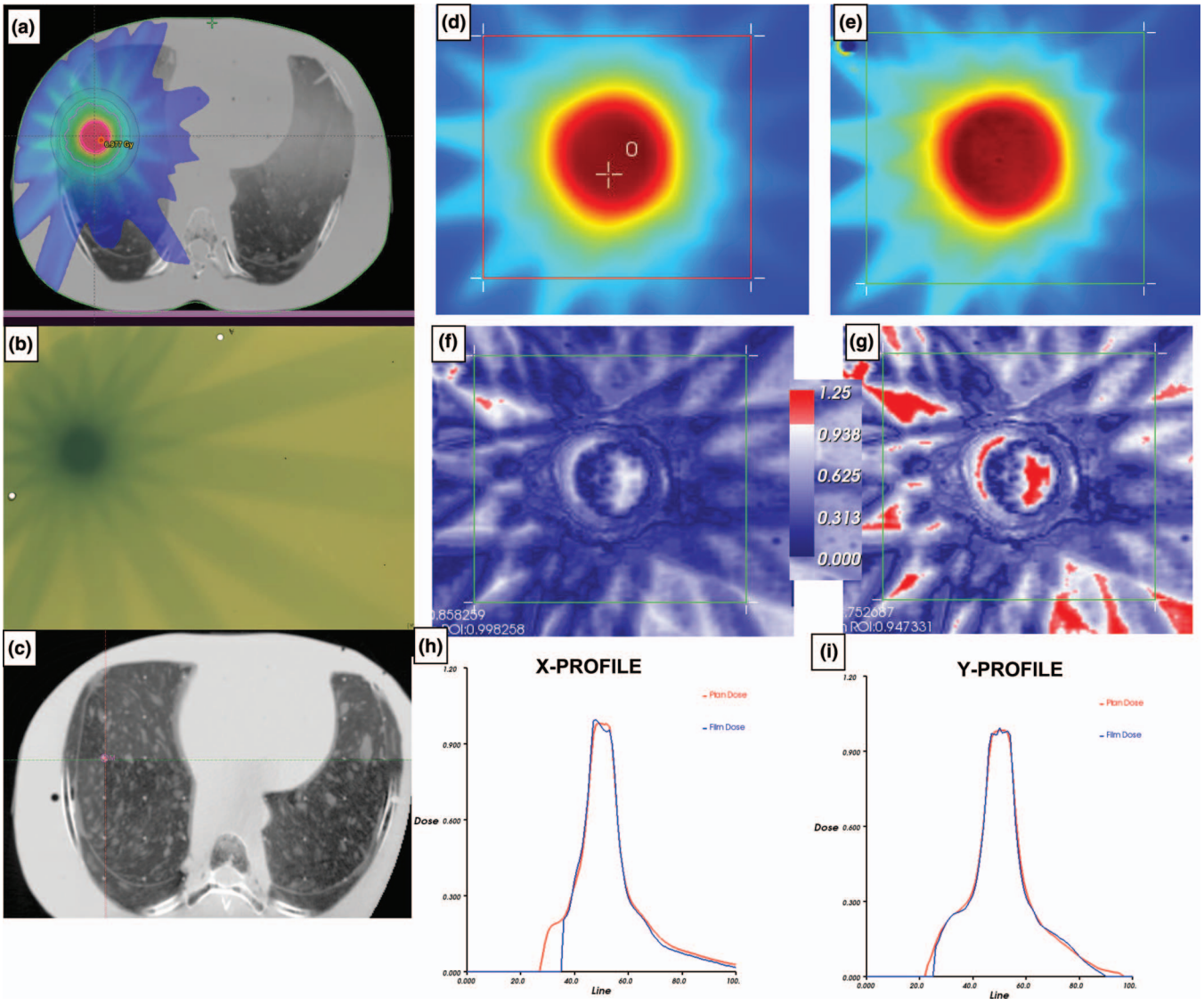

FIG. 8. End-to-end testing for a Rando thorax phantom for a TrueBeam machine. (a) Axial plane of the planned dose distribution, (b) exposed GAFCHROMIC™ EBT3 film from an axial plane near isocenter, (c) CBCT localization with the crosshairs indicating the BB location, (d) planned axial dose distribution at the level of film, (e) corresponding axial film dose distribution, (f) film gamma analysis results with 3% dose difference and 3 mm distance to agreement [99.8% of pixels passed within region of interest, with scale indicating gamma (unitless quantity)], (g) film gamma analysis results with 2% dose difference and 2 mm distance to agreement (94.7% of pixels passed within region of interest), (h) corresponding horizontal (X-dimension) and (i) vertical (Y-dimension) profiles for planned and delivered film doses.

arbitrary units), which agrees with what has been reported in the literature.[23,25]

Some systematic differences were also observed in the commissioning data. For example, HFHS1 MLC DLG values were ~0.4 mm less than the other institutions across all photon energies. However, these HFHS data of smaller magnitude demonstrated closer agreement to the DLG values presented in the recent work by Chang *et al.*[23] (i.e., mean DLGs for three TrueBeam machines at the same institution ranged from 0.71 to 0.96 mm for 6XFFF and 15 MV, respectively). On the other hand, Ong *et al.*[26] recently reported a DLG of 1.37 mm for 10XFFF, which was similar to the overall mean value across measured TrueBeams. All institutions in this work used the same DICOM plan files and measurement setup as defined by the manufacturer. Nevertheless, matched DLG values cannot be expected between institutions and different machines, namely, due to slight differences in MLC calibration, mechanical uncertainties, and construction discrepancies of the leaves.[22] It has been suggested that systematic differences in the DLG of ~0.6 mm may yield ~2% change in the equivalent uniform dose for standard head and neck IMRT plans.[27] The most complex TG-119 IMRT commissioning treatment plan results were illustrated for HFHS1 and 2. For the IMRT plan at the central core (low dose region), the composite point dose was 0.0056, while the TG-119 value for 10 institutions was 0.009 ± 0.025.[15] In the high dose region, 0.0088 was calculated as compared to the TG-119 result of -0.001 ± 0.036. Gafchromic film analysis of the high-dose region revealed ~99% pass rate at a gamma level of 3%/3 mm. Overall, strong agreement with reported TG-119 values gives confidence in

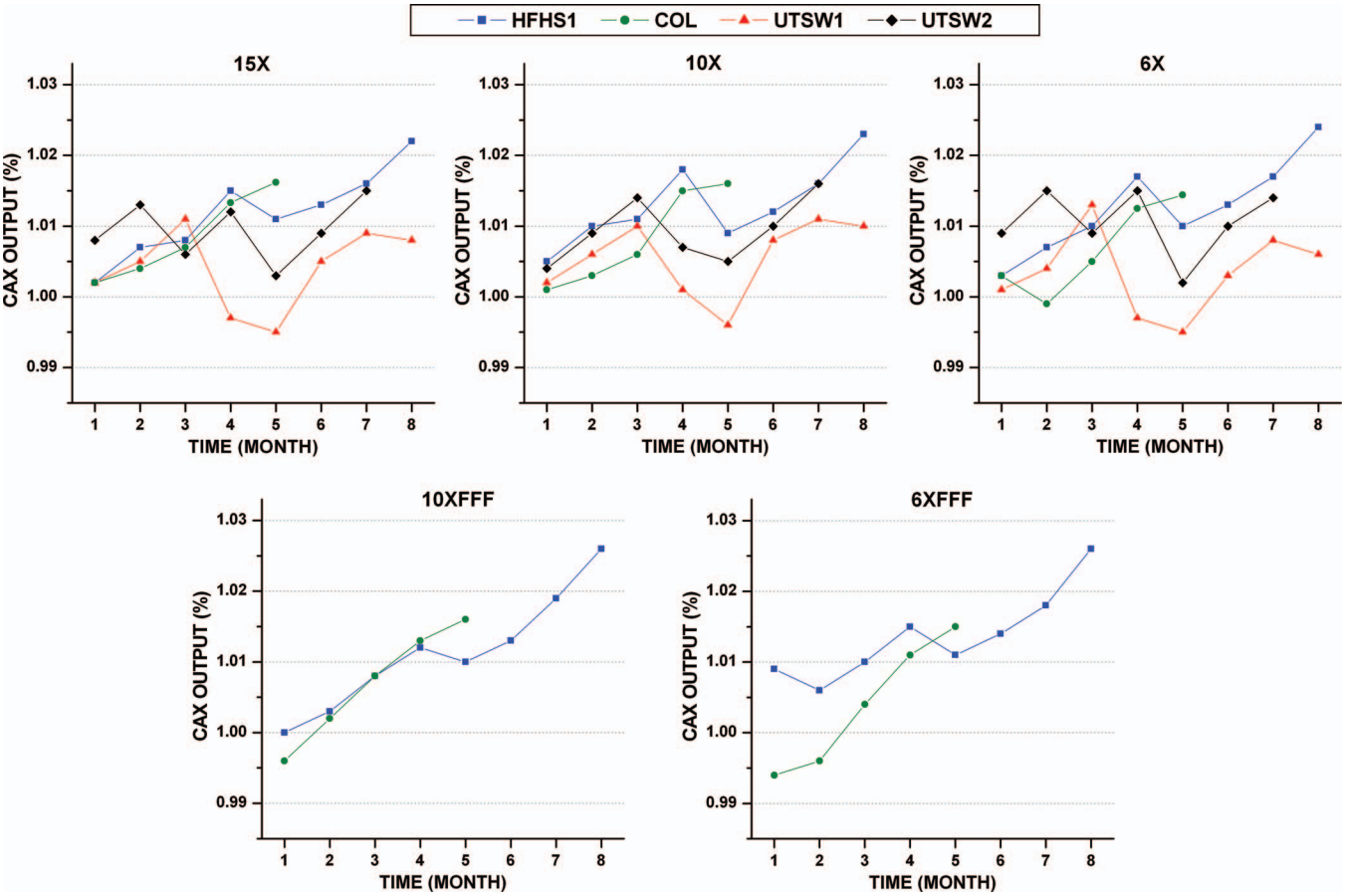

FIG. 9. Monthly central axis output measurements for all photons available on the TrueBeam units. Flattening filter free modes were not compatible with the record and verify system at UTSW, and were unavailable for comparison.

the TrueBeam IMRT commissioning and beam modeling process. While specific measurements were not repeated among beam energies to develop institution-specific confidence levels, a variety of plans were calculated for each photon energy to offer further assessment of initial IMRT verification.

Direct comparison for the 6XFFF TrueBeam RapidArc plan to TG-119 was not possible, as TG-119 does not provide confidence limits for arc therapy. Recently, a comprehensive multi-institutional study was conducted by the European TrueBeam Council that explored patient-specific plan verification for IMRT and RapidArc plans using TrueBeam FFF modes.[28] Detailed RapidArc commissioning was beyond the scope of this work, although references are available in the literature for other linear accelerators.[6,14]

Consistent results were demonstrated for the electron beam quality specifier (R_{50}) across four machines, with the largest difference occurring at 12 MeV (1.5 mm). Effective SSD measurements were in strong agreement for the two HFHS TrueBeams, whereas measurements for UTSW were lower in magnitude. Despite the dispersion in results between institutions shown in Fig. 7, particularly for the 6×6 cm^2, a similar spread of values was observed by Chang *et al.*[23] for three TrueBeam machines measured at the same institution, presumably with the same equipment (i.e., effective SSD for 6×6 cm^2 6 MeV range = 65.4–69.1 cm).

For end-to-end testing, one institution passed the RPC head and neck IMRT credentialing test to provide an independent verification of the entire treatment planning and delivery process. Notably, the mean displacement between planned and measured isodose lines was 0 mm, which was less than the average displacement summarized in TG-119 (1.1 ± 1.3 mm) for 10 institutions.[15] These results suggest that the treatment planning and delivery processes, including IMRT, were within practice guidelines.

Review of the monthly output measurements for all institutions suggested that periodic adjustment of machine output was necessary at all institutions. General upward drifts were observed over the first 6 months of clinical use. This phenomenon has been documented in the literature for other linacs, with steep upward output trends of up to 2% observed within the first 2–3 months postcommissioning, and stabilization occurring about 2–3 years later.[29] Such output drifts may be related to changes in the dose monitoring capabilities including drifts in measurement electronics and in the sealed monitor chambers.[29]

Despite having varied commissioning approaches and using different detectors, excellent agreement was found with all of the parameters measured at three institutions. This work highlights a variety of techniques used to achieve similar commissioning goals, and is by no means all-inclusive. For

example, no wedge results (profiles or wedge factors) were included in this work, largely because all three institutions performed only verification measurements for enhanced dynamic wedges for non-FFF photon modes (6X, 10X, and 15X). Other ways to strengthen this work would be to include more institutions in the analysis and to repeat some measurements to increase the overall fidelity of the reported values. Nevertheless, this multi-institutional data of five different TrueBeam machines provides useful comparison.

V. CONCLUSION

Overall, strong agreement was observed for all institutions, despite having varied equipment and acquisition techniques. This multi-institutional dataset may help other institutions embarking on TrueBeam commissioning, and is hoped to be of significant value to the medical physics community.

ACKNOWLEDGMENTS

Commissioning is an institutional effort, and sincere gratitude is extended to those who assisted during the commissioning process at each institution, particularly Chadd Smith, Jinkoo Kim, and Karen Chin at HFHS, Zeke Ramirez and Pam Lee at UTSW, and Kelly Stuhr and Leah Schubert at COL.

[a]Author to whom correspondence should be addressed. Electronic mail: churst2@hfhs.org

[1]J. Hrbacek, S. Lang, and S. Klock, "Commissioning of photon beams of a flattening filter-free linear accelerator and the accuracy of beam modeling using an anisotropic analytical algorithm," Int. J. Radiat. Oncol., Biol., Phys. **80**, 1228–1237 (2011).

[2]R. Nath, P. J. Biggs, F. J. Bova, C. C. Ling, J. A. Purdy, J. van de Geijn, and M. S. Weinhous, "AAPM code of practice for radiotherapy accelerators: Report of AAPM Radiation Therapy Task Group No. 45," Med. Phys. **21**, 1093–1121 (1994).

[3]I. J. Das, C.-W. Cheng, R. J. Watts, A. Ahnesjo, J. Gibbons, X. A. Li, J. Lowenstein, R. K. Mitra, W. E. Simon, and T. C. Zhu, "Accelerator beam data commissioning equipment and procedures: Report of the TG-106 of the Therapy Physics Committee of the AAPM," Med. Phys. **35**, 4186–4215 (2008).

[4]S. H. Benedict, K. M. Yenice, D. Followill, J. M. Galvin, W. Hinson, B. Kavanagh, P. Keall, M. Lovelock, S. Meeks, L. Papiez, T. Purdie, R. Sadagopan, M. C. Schell, B. Salter, D. J. Schlesinger, A. S. Shiu, T. Solberg, D. Y. Song, V. Stieber, R. Timmerman, W. A. Tome, D. Verellen, L. Wang, and F. F. Yin, "Stereotactic body radiation therapy: The report of AAPM Task Group 101," Med. Phys. **37**, 4078–4101 (2010).

[5]M. C. Schell, F. J. Bova, D. A. Larson, D. D. Leavitt, W. R. Lutz, E. B. Podgorsak, and A. Wu, *Stereotactic Radiosurgery; AAPM Report 54, Task Group 42* (American Institute of Physics, New York, 1995).

[6]D. G. Kaurin, L. E. Sweeney, E. I. Marshall, and S. Mahendra, "VMAT testing for an Elekta accelerator," J. Appl. Clin. Med. Phys. **13**(2) (2012).

[7]K. R. Winston and W. Lutz, "Linear accelerator as a neurosurgical tool for stereotactic radiosurgery," Neurosurgery **22**, 454–464 (1988).

[8]P. R. Almond, P. J. Biggs, B. M. Coursey, W. F. Hanson, M. S. Huq, R. Nath, and D. W. Rogers, "AAPM's TG-51 protocol for clinical reference dosimetry of high-energy photon and electron beams," Med. Phys. **26**, 1847–1870 (1999).

[9]F. Ponisch, U. Titt, O. N. Vassiliev, S. F. Kry, and R. Mohan, "Properties of unflattened photon beams shaped by a multileaf collimator," Med. Phys. **33**, 1738–1746 (2006).

[10]G. Kragl, S. af Wetterstedt, B. Knäusl, M. Lind, P. McCavana, T. Knöös, B. McClean, and D. Georg, "Dosimetric characteristics of 6 and 10 MV unflattened photon beams," Radiother. Oncol. **93**, 141–146 (2009).

[11]S. Dieterich and G. W. Sherouse, "Experimental comparison of seven commercial dosimetry diodes for measurement of stereotactic radiosurgery cone factors," Med. Phys. **38**, 4166–4173 (2011).

[12]Varian Medical Systems, "Eclipse Algorithms Reference Guide," P/N B503486R01B (2011). [http://myVarian.com].

[13]A. Boyer, P. Biggs, J. Galvin, E. Klein, T. LoSasso, D. Low, K. Mah, and C. Yu, "Basic applications of multileaf collimators," AAPM Radiation Therapy Committee Task Group No. 50 Report No. 72, 2001.

[14]C. C. Ling, P. Zhang, Y. Archambault, J. Bocanek, G. Tang, and T. Losasso, "Commissioning and quality assurance of RapidArc radiotherapy delivery system," Int. J. Radiat. Oncol., Biol., Phys. **72**, 575–581 (2008).

[15]G. A. Ezzell, J. W. Burmeister, N. Dogan, T. J. LoSasso, J. G. Mechalakos, D. Mihailidis, A. Molineu, J. R. Palta, C. R. Ramsey, B. J. Salter, J. Shi, P. Xia, N. J. Yue, and Y. Xiao, "IMRT commissioning: Multiple institution planning and dosimetry comparisons: A report from AAPM Task Group 119," Med. Phys. **36**, 5359–5373 (2009).

[16]J. Kim, S. Kim, M. Shaikh, H. Li, Y. Huang, N. Wen, C. Glide-Hurst, J. Jin, T. Nurushev, and I. J. Chetty, "Systematic evaluation of uncertainties associated with GAFCHROMIC EBT2 film dosimetry for 6MV photon beams," Med. Phys. **38**, 3524 (2011).

[17]F. M. Khan, K. P. Doppke, K. R. Hogstrom, G. J. Kutcher, R. Nath, S. C. Prasad, J. A. Purdy, M. Rozenfeld, and B. L. Werner, "Clinical electron-beam dosimetry: Report of AAPM Radiation Therapy Committee Task Group No. 25," Med. Phys. **18**, 73–109 (1991).

[18]F. M. Khan, *The Physics of Radiation Therapy* (Lippincott, Philadelphia, PA, 2003).

[19]J. Kim, N. Wen, J. Y. Jin, N. Walls, S. Kim, H. Li, L. Ren, Y. Huang, A. Doemer, K. Faber, T. Kunkel, A. Balawi, K. Garbarino, K. Levin, S. Patel, M. Ajlouni, B. Miller, T. Nurushev, C. Huntzinger, R. Schulz, I. J. Chetty, B. Movsas, and S. Ryu, "Clinical commissioning and use of the Novalis Tx linear accelerator for SRS and SBRT," J. Appl. Clin. Med. Phys. **13**, 3729 (2012).

[20]G. Videtic, A. Singh, and J. Chang, "A randomized phase II study comparing 2 stereotactic body radiation therapy (SBRT) schedules for medically inoperable patients with stage I peripheral non-small cell lung cancer. Radiation Therapy Oncology Group 0915."

[21]A. Molineu, D. S. Followill, P. A. Balter, W. F. Hanson, M. T. Gillin, M. S. Huq, A. Eisbruch, and G. S. Ibbott, "Design and implementation of an anthropomorphic quality assurance phantom for intensity-modulated radiation therapy for the Radiation Therapy Oncology Group," Int. J. Radiat. Oncol., Biol., Phys. **63**, 577–583 (2005).

[22]I. Chauvet, A. Petitfils, C. Lehobey, J. Y. Kristner, Y. Brunet, R. Lembrez, G. Gaboriaud, A. Mazal, S. Zefkili, and J. C. Rosenwald, "The sliding slit test for dynamic IMRT: A useful tool for adjustment of MLC related parameters," Phys. Med. Biol. **50**, 563–580 (2005).

[23]Z. Chang, Q. Wu, J. Adamson, L. Ren, J. Bowsher, H. Yan, A. Thomas, and F. F. Yin, "Commissioning and dosimetric characteristics of TrueBeam system: Composite data of three TrueBeam machines," Med. Phys. **39**, 6981–7018 (2012).

[24]G. P. Beyer, "Commissioning measurements for photon beam data on three TrueBeam linear accelerators, and comparison with Trilogy and Clinac 2100 linear accelerators," J. Appl. Clin. Med. Phys. **14**(1), (2013).

[25]Y. Wang, S. B. Easterling, and J. Y. Ting, "Ion recombination corrections of ionization chambers in flattening filter-free photon radiation," J. Appl. Clin. Med. Phys. **13**(5) (2012).

[26]C. L. Ong, W. F. A. R. Verbakel, M. Dahele, J. P. Cuijpers, B. J. Slotman, and S. Senan, "Fast arc delivery for stereotactic body radiotherapy of vertebral and lung tumors," Int. J. Radiat. Oncol., Biol., Phys. **83**, e137–e143 (2012).

[27]A. Rangel and P. Dunscombe, "Tolerances on MLC leaf position accuracy for IMRT delivery with a dynamic MLC," Med. Phys. **36**, 3304–3309 (2009).

[28]S. Lang, G. Reggiori, J. Puxeu Vaquee, C. Calle, J. Hrbacek, S. Klock, M. Scorsetti, L. Cozzi, and P. Mancosu, "Pretreatment quality assurance of flattening filter free beams on 224 patients for intensity modulated plans: A multicentric study," Med. Phys. **39**, 1351–1356 (2012).

[29]M. Kapanen, M. Tenhunen, T. Hämäläinen, P. Sipilä, R. Parkkinen, and H. Järvinen, "Analysis of quality control data of eight modern radiotherapy linear accelerators: The short- and long-term behaviours of the outputs and the reproducibility of quality control measurements," Phys. Med. Biol. **51**(14), 3581–3592 (2006).